COVID-19 Models and Model Fitting

Bernt Lie

University of South-Eastern Norway, Porsgrunn, Norway, Bernt.Lie@usn.no

Abstract

The paper discusses how to use cumulative confirmed infected numbers to find basic infection parameters. Next, an extension of the SEIR model, the SEICUR model from the literature (a renaming of the SEIRU model) is introduced, with details of how to compute the full set of model parameters, as well as the reproduction number R. A discussion is given of how the infection rate parameter relates to mitigation policy and various natural variations. Based on a simple mitigation model, an equivalent mitigation policy is found for Italy, Spain, and Norway. An indication of how to use feedback control theory to develop mitigation policy planning is given.
Keywords: COVID-19 models, deterministic models, model fitting, control relevance

1 Introduction

1.1 Background

The COVID-19[1] pandemic spread in 2020 initially caused fear, irrational hoarding of consumer goods, uncertainty about future food supply, and economic depression, but also spawned a renewed interest in epidemiology to understand how infections spread, and a massive effort in development of virus medicine and vaccines. Policy making and society saw challenges hardly faced before on how to adapt to the development in real time.

Data for the number of COVID-19 infected and deaths related to this, started to appear in January-February 2020. Initially, the number of infected and deaths were highly uncertain and underreported due to lack of reliable test procedures. Due to many asymptomatically infected, the true number of infected is still uncertain, while the number of deaths is more certain. Still, there is a discussion on whether people die *of* COVID-19 or *with* COVID-19. Relatively reliable sources suggest around 600 thousand deaths in USA as of this writing[2], while some report more than 900 thousand deaths in USA based on some estimate of underreporting[3].

A number of COVID-19 models have been developed since March 2020; many of them are vague on how to integrate data with the models, few discuss mitigation policy (hand cleaning, social distancing, etc.), how to design such policy under model uncertainty, and the effects of virus mutation and vaccination.

1.2 Previous work

Classical epidemiology models were developed in the decade following the "Spanish Flu". A renewed *public* interest in epidemic models started with the AIDS/HIV epidemic some decades ago; these models have been used to study other infectious diseases, e.g., (Brauer et al., 2019). (Lie, 2021) gives a brief overview of such general models from a process engineering point of view.

(Zlojutro et al., 2019) give a general framework, pre COVID-19, for border control to mitigate global outbreaks, and include stochastic models per country, with transport between countries by airlines. The *IHME COVID-19 Forecasting Team*[4] give a general overview of their model in (Reiner et al., 2021)[5]. An early study by Imperial College London[6] convinced the government in USA to take the epidemic more seriously. Many models have been provided on-line in web pages. A review of COVID-19 models is given by (Rahimi et al., 2021).

It is difficult to find models that are described completely, with model parameters. One such model is that of (López and Rodó, 2020), giving parameters for various regions in Spain. The SEIRU and SIRU models, (Liu et al., 2020b,a,c), are relatively; symbol R denotes *reported* cases instead of the conventional use of R as *recovered*. These SEIRU class models are macro models for each country, and have the *important advantage* over other models that the "reported" class equals the number of reported infected. Yet another model is that used by the Public Health Institute in Norway, (Øyvann, 2020), and probably several other centers for disease control (CDC) in Europe. In Norway, this model is posed for each municipality (possibly also for certain suburbs), and includes migration between each compartment — estimated from anonymized mobile phone locations.

A key parameter in all models is the infection rate. The infection rate is a problematic quantity which varies with natural phenomena and season, as well as mitigation pol-

[1] COVID-19 is the COrona VIrus Disease originating in 2019. The World Health Organization and Wikipedia.com both appear to write COVID-19 in all caps.

[2] https://www.worldometers.info/coronavirus/, https://coronavirus.jhu.edu/

[3] https://covid19.healthdata.org/united-states-of-america?view=cumulative-deaths&tab=trend

[4] The Institute for Health Metrics and Evaluation (IHME) is an independent global health research center at the University of Washington

[5] https://covid19.healthdata.org/united-states-of-america?view=cumulative-deaths&tab=trend

[6] https://www.imperial.ac.uk/mrc-global-infectious-disease-analysis/covid-19/covid-19-planning-tools/

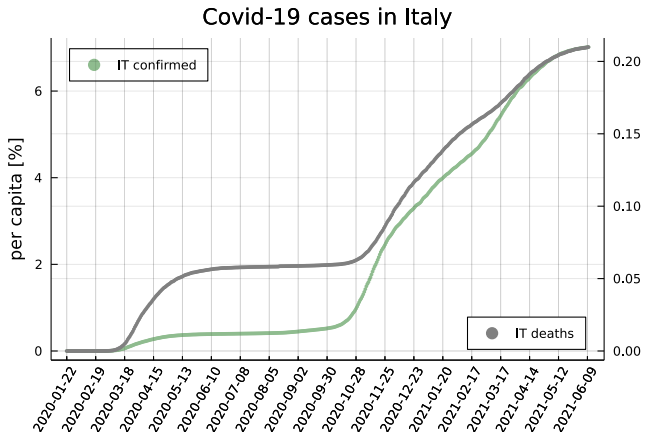

Figure 1. Cumulative number of confirmed infected in Italy vs. time (darkseagreen; left ordinate axis), and cumulative number of dead (grey; right ordinate axis).

icy and occurrence of mutations.

1.3 Scope

In Section 2, some available data are discussed, and basic model parameters are found. The SEICUR model is introduced (recasting of the SEIRU model), with procedures for finding model parameters. This model is constrasted to the Public Health Institute (PHI) of Norway. The infection rate parameter is related to mitigation policy, and expressions for reproduction number is given. In Section 3, the SEICUR model is fitted to data for Italy, Spain, and Norway. In Section 4, the results are discussed, and some conclusions are drawn.

All computations in the paper are carried out using language Julia, with packages `DifferentialEquations.jl`, (Rackauckas and Nie, 2017a), (Rackauckas and Nie, 2017b), (Rackauckas and Nie, 2018), `LsqFit.jl` for initial curve fitting, `BlackBoxOptim.jl` for equivalent mitigation policy fitting, and `Plots.jl` for plotting results.

2 Materials and Methods

2.1 COVID-19 data

Web page `https://github.com/octonion/COVID-19`, at folder `csse_covid_19_data`, subfolder `csse_covid_19_time_series`, file `time_series_covid19_confirmed_global.csv` provides daily updates of globally confirmed infected. Pre-treatment is required: some countries give regional data; others total data for the country. Here, we will focus on models for Norway, Italy, and Spain. Figure 1 shows cumulative number of infected and dead in Italy. Although it is possible to also model the rate of deaths, this is not done in this paper.

2.2 Initial evolution of $\mathfrak{C}$

Form of initial evolution Let $\mathfrak{C}$ denote the number of cumulative confirmed infected, which can be expressed as

$$\frac{\mathrm{d}\mathfrak{C}}{\mathrm{d}t} = \varphi \tag{1}$$

where φ is the rate at which people are confirmed infected. The actual expression for φ depends on the infection model. In the initial phase of an epidemic starting from the disease-free case, the rate at which people become confirmed infected increases exponentially

$$\varphi(t) = \varphi_0 \exp(\lambda \cdot (t - t_0)),$$

with $\lambda > 0$. Let $\Delta t \triangleq t - t_0$, $\Delta\mathfrak{C}(\Delta t) \triangleq \mathfrak{C}(t) - \mathfrak{C}(t_0)$, and $\chi_0 \triangleq \frac{\varphi_0}{\lambda}$, it follows that

$$\Delta\mathfrak{C}(\Delta t) = \chi_0 (\exp(\lambda \cdot \Delta t) - 1). \tag{2}$$

Parameters λ and φ_0 from time series of $\mathfrak{C}$ Assuming that time series data for $\Delta\mathfrak{C}(\Delta t)$ are known, we can tune χ_0 and λ to fit $\Delta\mathfrak{C}(\Delta t)$ to a function

$$\Delta\mathfrak{C}(\Delta t) = \chi_0 (\exp(\lambda \cdot \Delta t) - 1)$$

where we need to choose t_0, store the corresponding $\mathfrak{C}(t_0) = \mathfrak{C}_0$. Finally, we find φ_0 from $\varphi_0 = \lambda \cdot \chi_0$.

Parameters λ and φ_0 from $\mathfrak{C}$ in two data points If $\mathfrak{C}$ is known in two time instances t_0 and t_1, the slope of $\mathfrak{C}$ is known at t_0, $\Delta t = t_1 - t_0$, and the cumulative number of confirmed infected is *growing*,

$$\alpha \triangleq \frac{\Delta\mathfrak{C}/\Delta t}{\mathrm{d}\mathfrak{C}/\mathrm{d}t|_0} > 1,$$

it can be shown that λ is given by

$$\lambda = -\frac{\frac{1}{\alpha} + \mathscr{W}_{-1}\left(-\frac{1}{\alpha}\exp\left(-\frac{1}{\alpha}\right)\right)}{\Delta t}, \tag{3}$$

where $\mathscr{W}_{-1}(\cdot)$ is the lower branch of the Lambert W function.

With λ computed from Eq. 3, we find φ_0 as

$$\varphi_0 = \lambda \cdot \chi_0 = \left.\frac{\mathrm{d}\mathfrak{C}}{\mathrm{d}t}\right|_0. \tag{4}$$

The accuracy of this method of computing φ_0 and λ from two data points depends on how accurately $\left.\frac{\mathrm{d}\mathfrak{C}}{\mathrm{d}t}\right|_0$ can be found.

Parameters and initial values for Italy Data for Italy for the 9 d period February 23 – March 3, 2020 indicates relatively exponential growth for φ, leading to a good fit for $\mathfrak{C}(t)$, Figure 2.

The following procedures are used to estimate λ and φ_0:

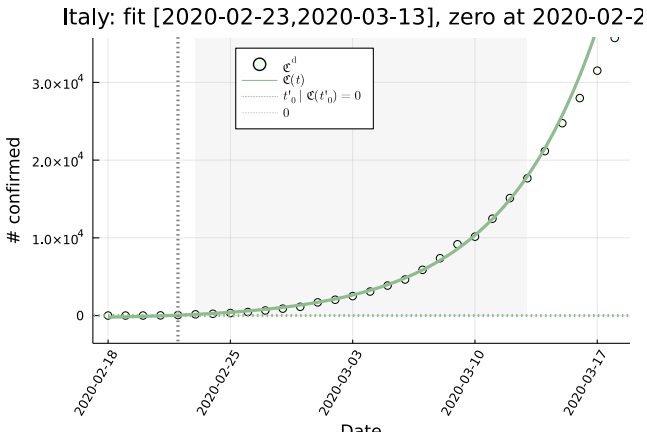

Figure 2. Fit of $\mathfrak{C}$ for Italy in the period February 23 – March 3, 2020.

Method 1 Fitting $\Delta\mathfrak{C}(\Delta t) = \chi_0(\exp(\lambda\cdot\Delta t)-1)$ to the data $\mathfrak{C}$. Computing φ_0 from $\varphi_0 = \lambda\cdot\chi_0$.

Method 2 Using the Lambert W approach, Eq. 3, to find λ, and next finding $\frac{\mathrm{d}\mathfrak{C}}{\mathrm{d}t}\big|_0$ found from fitting $\Delta\mathfrak{C}(\Delta t) = \chi_0(\exp(\lambda\cdot\Delta t)-1)$, and computing φ_0 according to Eq. 4 as $\varphi_0 = \frac{\mathrm{d}\mathfrak{C}}{\mathrm{d}t}\big|_0$.

Method 3 Using the Lambert W approach to find λ with $\frac{\mathrm{d}\mathfrak{C}}{\mathrm{d}t}\big|_0 \approx \frac{\mathfrak{C}(t_1)-\mathfrak{C}(t_0)}{t_1-t_0}$ where $t_1 = t_0+1$ and t_0 is February 23, 2020; $\varphi_0 = \frac{\mathrm{d}\mathfrak{C}}{\mathrm{d}t}\big|_0$.

Method 4 Using the Lambert W approach to find λ with $\frac{\mathrm{d}\mathfrak{C}}{\mathrm{d}t}\big|_0$ found by fitting a 3rd order polynomial to $\mathfrak{C}$ and computing the initial derivative of $\mathfrak{C}$; $\varphi_0 = \frac{\mathrm{d}\mathfrak{C}}{\mathrm{d}t}\big|_0$.

Method 5 Using the Lambert W approach to find λ with $\frac{\mathrm{d}\mathfrak{C}}{\mathrm{d}t}\big|_0$ found by fitting a 2nd order polynomial to $\log\mathfrak{C}$ and computing the initial derivative of $\mathfrak{C}$; $\varphi_0 = \frac{\mathrm{d}\mathfrak{C}}{\mathrm{d}t}\big|_0$.

The results show that Methods 1, 2, 3, and 5 give relatively similar results, while Method 4 gives a rather different result. The reason is that polynomial fit to $\mathfrak{C}$ gives a poor estimate of the initial derivative. Also for other countries, Method 1 appears to give the most reliable results, followed by Method 2. Here, we report the parameters from Method 1.

Summary parameters and initial values Table 1 gives a summary of fitted parameters t_0, t_1, $\mathfrak{C}_0$, φ_0, and λ for Italy, Spain, and Norway, based on Method 1.

2.3 SEICUR model

2.3.1 Reaction mechanism

An SEIR model with the infected I population extended to (I,C,U) was proposed for COVID-19 in (Liu et al., 2020b)[7], Figure 3.

The proposed mechanism implies that *susceptibles* S are infected by some "pre-infected" I and the non-quarantined *unconfirmed* U leading to the *exposed* phase E, which is infected but not yet infectious. These exposed E then are converted to the "pre-infected" I class, which then either become more serious cases and are *confirmed* infected C, or stay as *unconfirmed* U. Finally, the confirmed infected and the unconfirmed end up in the *recovered* population R (which includes those who die). We will refer to this model as the SEICUR model.

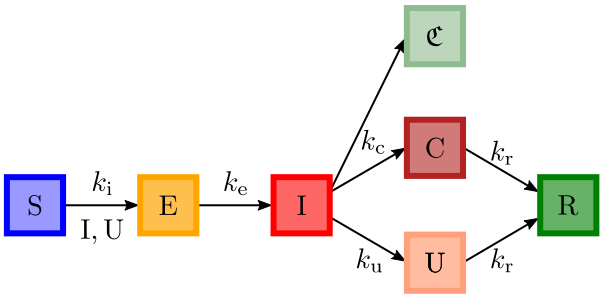

Figure 3. Flow of SEICUR reactions.

The following mechanism describes the reactions:

$$\begin{aligned}
\mathscr{E}_\mathrm{i}&:\mathrm{S}\overset{\mathrm{I+U}^{k_\mathrm{i}}}{\rightarrow}\mathrm{E}, & r_\mathrm{i} &= k_\mathrm{i}\left(\check{I}+\check{U}\right)\check{S}\\
\mathscr{E}_\mathrm{e}&:\mathrm{E}\rightarrow^{k_\mathrm{e}}\mathrm{I}, & r_\mathrm{e} &= k_\mathrm{e}\check{E}\\
\mathscr{E}_\mathrm{c}&:\mathrm{I}\rightarrow^{k_\mathrm{c}}\mathrm{C}, & r_\mathrm{c} &= k_\mathrm{c}\check{I}\\
\mathscr{E}_\mathrm{u}&:\mathrm{I}\rightarrow^{k_\mathrm{u}}\mathrm{U}, & r_\mathrm{u} &= k_\mathrm{u}\check{I}\\
\mathscr{E}_\mathrm{cr}&:\mathrm{C}\rightarrow^{k_\mathrm{r}}\mathrm{R}, & r_\mathrm{cr} &= k_\mathrm{r}\check{C}\\
\mathscr{E}_\mathrm{ur}&:\mathrm{U}\rightarrow^{k_\mathrm{r}}\mathrm{R}, & r_\mathrm{ur} &= k_\mathrm{r}\check{U}.
\end{aligned}$$

We introduce

$$\begin{aligned}
k_\mathrm{cu} &= k_\mathrm{c}+k_\mathrm{u}\\
k_\mathrm{c} &= \eta k_\mathrm{cu}.
\end{aligned}$$

Thus, specifying k_cu and η, we can find

$$\begin{aligned}
k_\mathrm{c} &= \eta k_\mathrm{cu}\\
k_\mathrm{u} &= (1-\eta)\,k_\mathrm{cu}.
\end{aligned}$$

The model assumes that the total population is fixed, and that a preliminary fitting to find ϕ_0 and λ has been carried out, Table 1. In the model fitting, the cumulative number of confirmed infected are used as observation y, i.e.,

$$y(t) = \mathfrak{C}(t)$$

where

$$\frac{\mathrm{d}\mathfrak{C}}{\mathrm{d}t} = k_\mathrm{c}I$$

with $\mathfrak{C}(t_0)$ assumed known. Thus, $\varphi = k_\mathrm{c}I$ in Eq. 1.

In the initial phase of infection spread before confirmed cases, it can be questioned whether members of the C class *quarantine*. Thus, one could consider that also members of compartment C participate in the infection. We will neglect this possibility here.

[7]The reference uses symbols (I,R,U); here, R ("registered") has been changed to C ("confirmed") to observe the classic meaning of R as "recovered")

Table 1. Values for t_0, t_1, $\mathfrak{C}_0$, φ_0 and λ for some countries. Parenthesis after dates t_0 and t_1 indicates the element number in the times series for the data. Population size N taken from `https://www.worldometers.info/coronavirus/` ca. April 2020.

Country	t_0	t_1	$\mathfrak{C}_0$	φ_0	λ	N
Italy	2020-02-23 (33)	2020-03-14 (52)	155	112	0.178	60443857
Spain	2020-02-24 (34)	2020-03-13 (51)	2	6.09	0.281	46758424
Norway	2020-02-27 (37)	2020-03-14 (52)	1	2.73	0.318	5429635

2.3.2 Approximate initial response

With the initial number of susceptibles $S(t_0)$ having a value close to the total population N, $S(t_0) \approx N$, and $S(t_0)$ being more or less constant in the first phase of the epidemic, the dynamic model can be approximated with a linear model with $X = (S,E,I,C,U,R)$ for "small" $(t-t_0)$,

$$\frac{\mathrm{d}X}{\mathrm{d}t} \approx MX.$$

Matrix M has two zero columns, thus has two eigenvalues in the origin; these reflect the approximate pure integrator of S and the true pure integrator for R. It thus suffices to consider subsystem $X' = (E,I,C,U)$ when considering infection growth:

$$\frac{\mathrm{d}X'}{\mathrm{d}t} = \underbrace{\begin{pmatrix} -k_\mathrm{e} & k_\mathrm{i} & 0 & k_\mathrm{i} \\ k_\mathrm{e} & -k_\mathrm{cu} & 0 & 0 \\ 0 & k_\mathrm{c} & -k_\mathrm{r} & 0 \\ 0 & k_\mathrm{u} & 0 & -k_\mathrm{r} \end{pmatrix}}_{M'} X'. \tag{5}$$

The structure of the system causes the single, positive eigenvalue λ of M' to dominate the dynamics during growth, with solutions $X'_i(t)$ for the elements of X':

$$X'_i(t) = \exp(\lambda(t-t_0)) X'_{i,0}. \tag{6}$$

2.3.3 Parameters and initial states

Parameters φ and λ are as found in Section 2.2, where $\varphi = k_\mathrm{c} I$ for the SEICUR model.

Assuming that k_cu, η, k_e, and k_r are *known*, and

$$k_\mathrm{c} = \eta k_\mathrm{cu} \tag{7}$$
$$k_\mathrm{u} = k_\mathrm{cu} - k_\mathrm{c}, \tag{8}$$

I_0 can be found from $k_\mathrm{c} I_0 = \varphi_0$ and known k_c,

$$I_0 = \frac{\varphi_0}{k_\mathrm{c}}. \tag{9}$$

Inserting the assumed solutions of Eq. 6 into the linearized differential equation Eq. 5 while cancelling the common term $\exp(\lambda(t-t_0))$, this leads to:

$$\lambda E_0 \approx k_\mathrm{i}(I_0 + U_0) - k_\mathrm{e} E_0 \tag{10}$$
$$\lambda I_0 \approx k_\mathrm{e} E_0 - k_\mathrm{cu} I_0 \tag{11}$$
$$\lambda C_0 \approx k_\mathrm{c} I_0 - k_\mathrm{r} C_0 \tag{12}$$
$$\lambda U_0 \approx k_\mathrm{u} I_0 - k_\mathrm{r} U_0. \tag{13}$$

The three last of these, Eqs. 11–13 can be solved wrt. E_0, C_0, and U_0 to give

$$E_0 = \frac{\lambda + k_\mathrm{cu}}{k_\mathrm{e}} I_0 \tag{14}$$
$$C_0 = \frac{k_\mathrm{c} I_0}{\lambda + k_\mathrm{r}} \tag{15}$$
$$U_0 = \frac{k_\mathrm{u} I_0}{\lambda + k_\mathrm{r}}. \tag{16}$$

The first one, Eq. 10, can be solved wrt. k_i to give

$$k_\mathrm{i} = \frac{(\lambda + k_\mathrm{e}) E_0}{I_0 + U_0}. \tag{17}$$

By assuming zero recovered, $R_0 = 0$, and known population N, we can compute the initial value of S:

$$S_0 = N - E_0 - I_0 - C_0 - U_0 - R_0. \tag{18}$$

2.3.4 Reproduction number

Using the *Next-Generation Approach*, (Lie, 2021), write $M' = F - V$. Making V lower triangular,

$$M' = \underbrace{\begin{pmatrix} 0 & k_\mathrm{i} & 0 & k_\mathrm{i} \\ 0 & 0 & 0 & 0 \\ 0 & 0 & 0 & 0 \\ 0 & 0 & 0 & 0 \end{pmatrix}}_{=F} - \underbrace{\begin{pmatrix} k_\mathrm{e} & 0 & 0 & 0 \\ -k_\mathrm{e} & k_\mathrm{cu} & 0 & 0 \\ 0 & -k_\mathrm{c} & k_\mathrm{r} & 0 \\ 0 & -k_\mathrm{u} & 0 & k_\mathrm{r} \end{pmatrix}}_{=V}, \tag{19}$$

this gives the simplest Next-Generation Matrix; here, both F and V^{-1} are *positive* matrices. The Next-Generation Matrix N is

$$N = FV^{-1}$$
$$\Downarrow$$
$$N = \begin{pmatrix} \frac{k_\mathrm{i}}{k_\mathrm{cu}}\left(1 + \frac{k_\mathrm{u}}{k_\mathrm{r}}\right) & \frac{k_\mathrm{i}}{k_\mathrm{cu}}\left(1 + \frac{k_\mathrm{u}}{k_\mathrm{r}}\right) & 0 & \frac{k_\mathrm{i}}{k_\mathrm{r}} \\ 0 & 0 & 0 & 0 \\ 0 & 0 & 0 & 0 \\ 0 & 0 & 0 & 0 \end{pmatrix}.$$

N has 3 eigenvalues in the origin, and one positive eigenvalue, which is the spectral radius:

$$\rho(N) = \frac{k_\mathrm{i}}{k_\mathrm{cu}}\left(1 + \frac{k_\mathrm{u}}{k_\mathrm{r}}\right) = \frac{k_\mathrm{i}}{k_\mathrm{r}}\left(1 - \eta + \frac{k_\mathrm{r}}{k_\mathrm{cu}}\right).$$

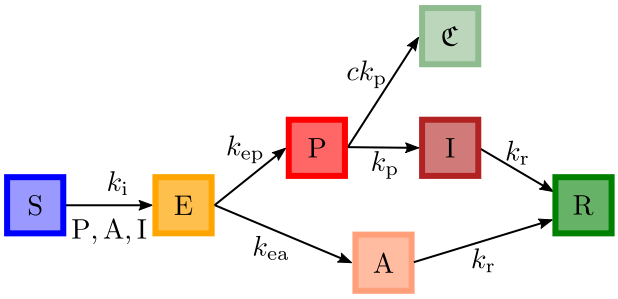

Figure 4. Flow of SEPIAR reactions.

We choose the following expression for R:

$$\mathsf{R} \triangleq \frac{k_\mathrm{i}}{k_\mathrm{r}}\left(1-\eta+\frac{k_\mathrm{r}}{k_\mathrm{cu}}\right), \tag{20}$$

which is the same as proposed in (Liu et al., 2020a).

(Sanche et al., 2020) cite initial estimates of R_0 for COVID-19 to be in the range $[2.2, 2.7]$.This number varies with location and time (mutations). The Delta mutant reportedly has R_0=6,[8] or perhaps even up to 8.

2.4 The Norwegian PHI model

The Publich Health Institute of Norway operates with what can be termed the SEPIAR model, Figure 4.

Here, P is a pre-symptomatic infectious stage, I is the symptomatic, infectious stage, and A is an asymptomatic yet slightly infectious stage. This is essentially a slightly extended SEIR model where I is (P, I, A). Numbers are provided for the various reaction constants.

The key difficulty with this model is that it does not directly correlate confirmed cases $\mathfrak{C}$ to the states; in Figure 4, it is indicated that $\frac{\mathrm{d}\mathfrak{C}}{\mathrm{d}t} = ck_\mathrm{p}P$, but constant c is unknown.

2.5 Variation in infection rate

The infection rate k_i is uncertain, and will also vary due to:

1. Mitigation effects: (a) Hygiene, (b) Social distancing, (c) Use of face mask, (d) Quarantining, (e) Closing spaces with loud talk = reducing spreading by saliva/aerosols.

2. Meteorological effects: (a) Increased humidity causes aeorosols/saliva droplets to travel shorter, (b) Stronger solar irradiation/higher temperature kills virus faster; (Wu et al., 2020).

3. Health + sociology: (a) Age/co-morbidity: old people/with co-morbidity are more affected by COVID-19, (b) Genetic effects: blood type, etc. may influence infection rate, (c) Immune system status, (d) Life/behavioral patterns.

4. Mutations.

[8] Dr. Tim Spector: https://youtu.be/OHBua3aXQ7c

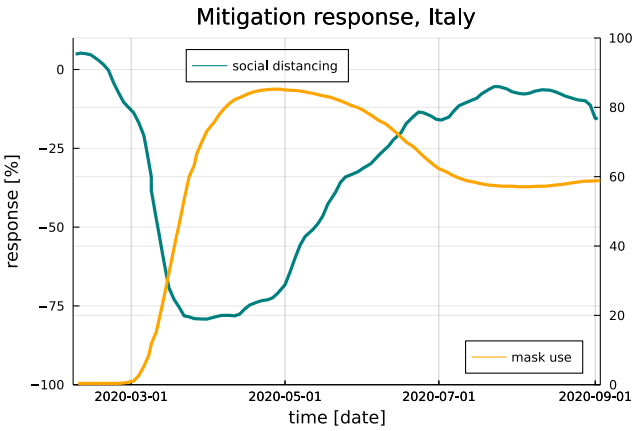

Figure 5. Social distancing (teal color, left ordinate) and mask (gold color, right ordinate) use in Italy, according to model of `https://covid19.healthdata.org/global?view=total-deaths&tab=trend`. Screen capture data converted to time series using WebPlotDigitizer, `https://automeris.io/WebPlotDigitizer/`.

Ideally, vaccination does not change the infection rate.[9] Instead, vaccination reduces the number of people susceptible to infection, see expression for infection rate r_i in Section 2.3.1.

2.6 Mitigation

Mitigation policies utilize effects that reduce infection rate. Typical examples are hygiene, social distancing, face mask use, quarantining, etc. The mitigation policy consists of recommendations or enforcing of law from the government, denoted $u(t)$, and this leads to a response from the public, denoted $x(t)$. For a better description, we might also include seasonal quantities (humidity, etc.), virus mutation, etc., as a *disturbance* $w(t)$ to a description.

Figure 5 proposes response in social diatancing and face mask use in Italy in the first 6 months of the COVID-19 pandemic. It is not clear whether these response data are based on actual observations, or based on some vague estimates.

A more formal description of how the mitigation policy u and disturbance variable w with response x transforms itself into an infection rate k_i, would be

$$\frac{\mathrm{d}x}{\mathrm{d}t} = f(x,u,w) \tag{21}$$

$$k_\mathrm{i} = g(x,u)\,. \tag{22}$$

Here, x is some state which describes the dynamics of the change of k_i, and may include people's inertia towards taking measures into use, and the tendency that people get tired of the measures and want to get back to normal life. The model with $f(x,u,w)$ and $g(x,u)$ could be found through some system identification technique when u, to some degree w, and k_i are known.

[9] ...assuming that vaccinated are immune — experience has shown some cases of breahthrough infection of vaccinated.

In principle, we could add *outputs* in addition to k_i, such as social distancing and mask use as in Figure 5, or other quantities such as humidity, etc.: this would help to give a more accurate mitigation model.

As an *alternative* to using system identification to fit a model from known mitigation policy u and disturbance w to known outputs, we could find some *equivalent* mitigation policy u_fm by postulating a fixed model structure, e.g.,

$$\frac{\mathrm{d}x}{\mathrm{d}t} = \frac{1}{T_\mathrm{m}}(u_\mathrm{fm} - x) \tag{23}$$

$$k_\mathrm{i} = k_\mathrm{i}^0 x, \tag{24}$$

and compute which input sequence u_fm gives a good model fit to confirmed cases. Here, T_m is the *mitigation* time constant, typically chosen to be 7–10 d. It follows that such an *equivalent* mitigation policy u_fm will include seasonal variations in infection rate, as well as the effect of virus mutation, etc. In other words, by comparing an equivalent mitigation policy u_fm from two different time instances, or in two different countries, we can not directly related u_fm to a specific level of social distancing, mask use, etc.: a value of $u_\mathrm{fm} = 0.5$ in June 2020 could imply a different level of social activity than a level of $u_\mathrm{fm} = 0.5$ in February 2021.

In the normal, pre COVID-19 situation with $u_\mathrm{fm} = 1$, x will asymptotically approach $x = 1$, and $k_\mathrm{i} \to k_\mathrm{i}^0$. As u_fm becomes smaller and smaller due to a low social contact mitigation policy, x will asymptotically approach a smaller and smaller value until it reaches value $x = 0$ for zero social contact. For that case, $k_\mathrm{i} \to 0$, which means that the reaction rate $\propto k_\mathrm{i}$ approaches zero. In the work of (Liu et al., 2020c), etc., the assumption of $x \to 0$ is assumed, which is unrealistic. In a realistic mitigation effect, we need to take into account a time varying mitigation policy u_fm.

3 Model Fitting

3.1 Initial evolution

Simulation of the initial (unmitigated) case of Italy using the SEICUR model is depicted in Figure 6.

As Figure 6 shows, the initial model reponse in $\mathfrak{C}$ fits the data $\mathfrak{C}^\mathrm{d}$ quite well, which should be expected: the model parameters were found by fitting the model to the initial data.

Based on the initial fitting, this gives a basic reproduction number of $\mathsf{R}_0 = 3.2$ for Italy. Similar numbers for Spain and Norway are found to be $\mathsf{R}_0 = 4.7$ and $\mathsf{R}_0 = 5.4$, respectively.

3.2 Fitted mitigation policy

3.2.1 Case Norway

It is possible to propose a "fitted" mitigation policy u_fm such that good correspondence model and confirmed infection cases is achieved. The fitted policy is depicted in Figure 7.

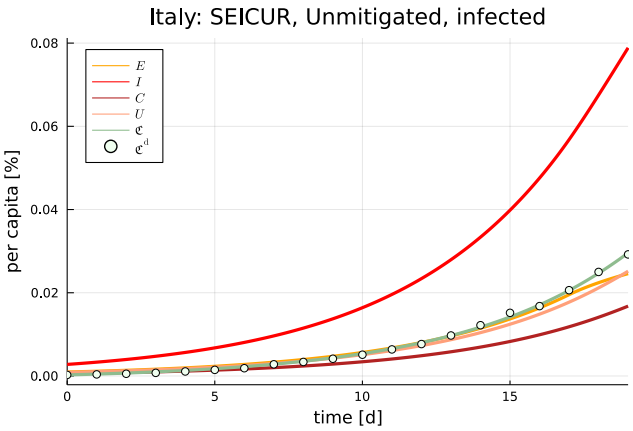

Figure 6. Initial (unmitigated) evolution according to the SEICUR model for Italy.

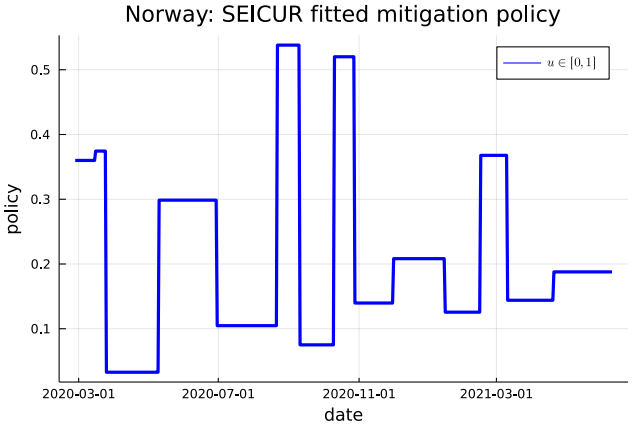

Figure 7. Fitted mitigation policy tuned to SEICUR model for Norway.

The resulting SEICUR model simulation with comparison to cumulative confirmed infections is shown in Figure 8. It may also be instructive to compare the smoothed 7-day avareage $\frac{\mathrm{d}\mathfrak{C}}{\mathrm{d}t}\big|_\mathrm{smooth}$ with $k_\mathrm{c} I$, Figure 9. As seen, this gives very good model fit in $\mathfrak{C}$, and decent fit in $\frac{\mathrm{d}\mathfrak{C}}{\mathrm{d}t}\big|_\mathrm{smooth}$.

An important comment is that vaccination started in Norway (and in Europe) in early 2021. In the above fitting, vaccination has not been taken into account, and thus the equivalent mitigation policy of Figure 7 and subsequent figures for Italy and Spain includes the effect of vaccination. If vaccination has had an important role for avoiding infection spread, including vaccination in the model should have lead to a more relaxed mitigation policy.

3.2.2 Case: Italy

The fitted policy is depicted in Figure 10.

The resulting SEICUR model simulation with comparison to cumulative confirmed infections is shown in Figure 11.

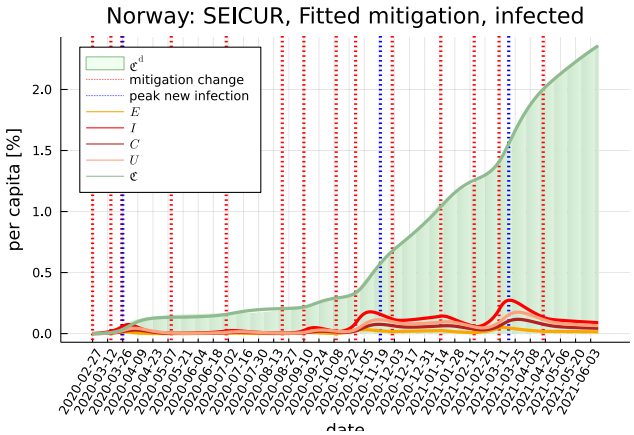

Figure 8. SEICUR model simulation with fitted mitigation policy as in Figure 7.

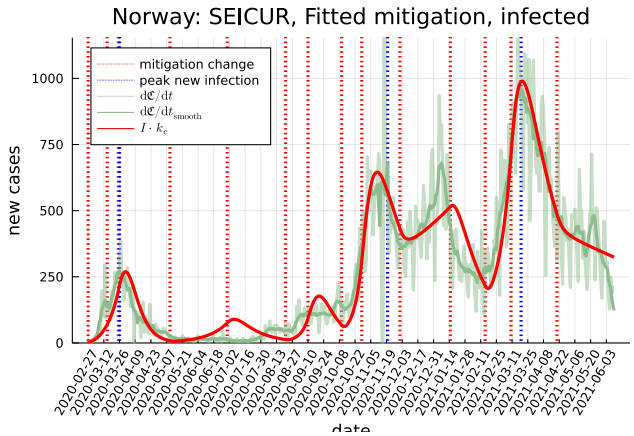

Figure 9. SEICUR model simulation with fitted mitigation policy as in Figure 7.

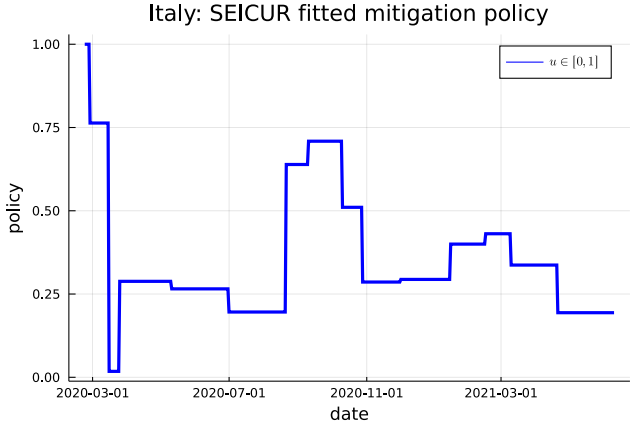

Figure 10. Fitted mitigation policy tuned to SEICUR model for Italy.

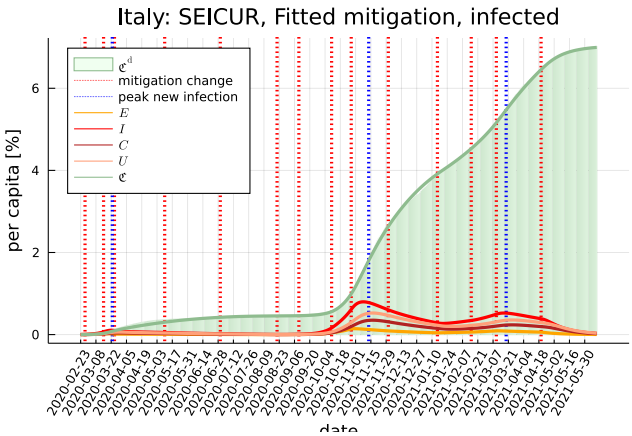

Figure 11. SEICUR model simulation with fitted mitigation policy as in Figure 10.

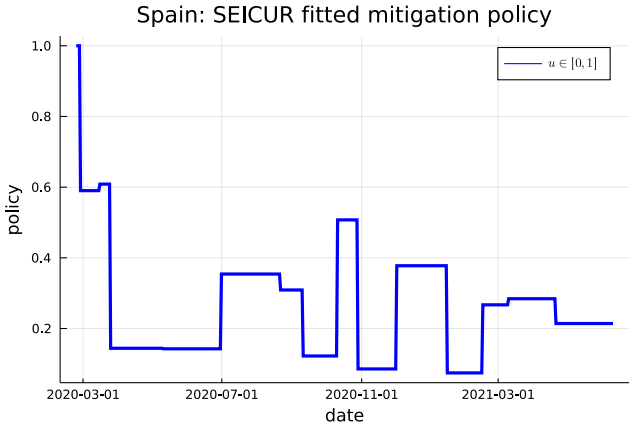

Figure 12. Fitted mitigation policy tuned to SEICUR model for Spain.

3.2.3 Case: Spain

The fitted policy is depicted in Figure 12.

The resulting SEICUR model simulation with comparison to cumulative confirmed infections is shown in Figure 13.

4 Discussion and conclusions

An overview has been given of a specific COVID-19 model of (Liu et al., 2020a), here denoted the SEICUR model. The minor advantage of this model over the Norwegian Public Health Institute model is related to the latter's lack of specifying how states related to confirmed cases. A number of methods to fit basic parameters φ_0 and λ to cumulative confirmed cases is given. Next, with a given model structure and some predetermined parameters from clinical data, a discussion on how to find the remaining model parameters is given, including k_i^0, from φ_0 and λ. Simulation of the model in an initial phase confirms that the model fit is adequate. An original contribution of the paper is the generalization of the initial model fit Eq. 2 to be independent of the model. Another contribution is the use of the Lambert W approach to estimate

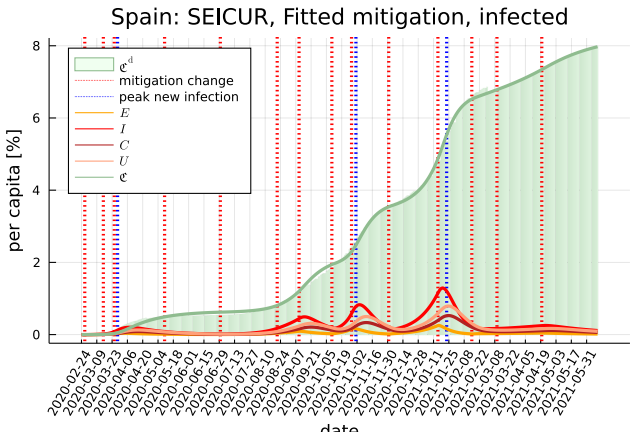

Figure 13. SEICUR model simulation with fitted mitigation policy as in Figure 12.

parameters λ and φ_0. These initial data have been fitted for Norway, and re-fitted for Italy and Spain. Also, the procedure of finding model-dependent parameters (k_i) and initial states (I_0, E_0, C_0, E_0) has been streamlined compared to the original papers. A detailed derivation of the reproduction model is given.

For extended periods of time after the initial phase, mitigation policy, seasonal changes, and virus mutation makes it necessary to add some modification to the infection rate constant k_i. Here, infection rate constant modification is done via an equivalent mitigation policy which is found by fitting the model to data for cumulative confirmed cases. The result is a very good fit. The results also indicate that the fit to the (averaged) daily new confirmed cases is less good, which should be expected: using cumulative data always smooths the information.

The formulation of the effect of a *fitted* mitigation policy on the infection rate constant is new, and the actual fitting of this policy for countries Norway, Italy, and Spain is new. The fitted mitigation policy at the current time could be used in conjunction with model prediction over a future horizon to design a feedback controller which could compute an advice on future mitigation policy, e.g., using Model Predictive Control. Because of the uncertainty in the computed equivalent mitigation policy u due to seasonal variations, etc., such a controller will be prone to a certain level of uncertainty.

References

Fred Brauer, Carlos Castillo-Chavez, and Zhilan Feng. *Mathematical Models in Epidemiology*. Number 69 in Texts in Applied Mathematics. Springer, New York, 2019. ISBN 978-1-4939-9826-5.

Bernt Lie. Epidemiological Models and Process Engineering. In *Proceedings, SIMS EUROSIM 2021, Oulu Finland, September 21–23*, 2021.

Z. Liu, P. Magal, O. Seydi, and G. Webb. A COVID-19 epidemic model with latency period. *Infectious Disease Modelling*, 5: 323–337, 2020a. doi:10.1016/j.idm.2020.03.003.

Zhihua Liu, Pierre Magal, Ousmane Seydi, and Glenn Webb. A model to predict covid-19 epidemics with applications to south korea, italy and spain. *SIAM News*, 2020b. https://sinews.siam.org/Details-Page/a-model-to-predict-covid-19-epidemics-with-applications-to-south-korea-italy-and-spain.

Zhihua Liu, Pierre Magal, and Glenn F Webb. Predicting the number of reported and unreported cases for the COVID-19 epidemics in china, south korea, italy, france, germany and united kingdom. apr 2020c. doi:10.1101/2020.04.09.20058974.

Leonardo López and Xavier Rodó. A modified SEIR model to predict the COVID-19 outbreak in Spain and Italy: simulating control scenarios and multi-scale epidemics. *Results in Physics*, 2020. doi:10.1016/j.rinp.2020.103746. URL `https://pubmed.ncbi.nlm.nih.gov/33391984/`.

Stig Øyvann. Jakten på en presis beskrivelse av epidemien. *Computerworld*, 38(6):26–30, December 2020.

Christopher Rackauckas and Qing Nie. DifferentialEquations.jl — A Performant and Feature-Rich Ecosystem for Solving Differential Equations in Julia. *Journal of Open Research Software*, 5(15), 2017a. doi:10.5334/jors.151.

Christopher Rackauckas and Qing Nie. Adaptive methods for stochastic differential equations via natural embeddings and rejection sampling with memory. *Discrete and continuous dynamical systems. Series B*, 22(7):2731, 2017b.

Christopher Rackauckas and Qing Nie. Stability-Optimized High Order Methods and Stiffness Detection for Pathwise Stiff Stochastic Differential Equations. *arXiv:1804.04344 [math]*, 2018. URL `http://arxiv.org/abs/1804.04344`.

Iman Rahimi, Fang Chen, and Amir H. Gandomi. A review on COVID-19 forecasting models. *Neural Computing and Applications*, 2021. doi:https://doi.org/10.1007/s00521-020-05626-8.

Jr. Reiner, Robert C., Ryan M. Barber, James K. Collins, and more. Modeling COVID-19 scenarios for the United States. *Nature Medicine*, 27:94–105, 2021. doi:https://doi.org/10.1038/s41591-020-1132-9.

Steven Sanche, Yen Ting Lin, Chonggang Xu, Ethan Romero-Severson, Nick Hengartner, and Ruian Ke. High Contagiousness and Rapid Spread of Severe Acute Respiratory Syndrome Coronavirus 2. *Emerging Infectious Diseases*, 26(7), July 2020. ISSN 1080-6059. URL `https://wwwnc.cdc.gov/eid/article/26/7/20-0282_article`.

Yu Wu, Wenzhan Jing, Jue Liu, Qiujue Ma, Jie Yuan, Yaping Wang, Min Du, and Min Liu. Effects of temperature and humidity on the daily new cases and new deaths of COVID-19 in 166 countries. *Science of the Total Environment*, 729(139051), August 2020. doi:https://doi.org/10.1016/j.scitotenv.2020.139051.

Aleksa Zlojutro, David Rey, and Lauren Gardner. A decision-support framework to optimize border control for global outbreak mitigation. *Scientific Reports*, (2216), 2019. doi:https://doi.org/10.1038/s41598-019-38665-w.